Reprinted from Nature, Vol. 328, No. 6129, pp. 391-395, 30 July 1987

Observed beaming of terrestrial myriametric radiation

Dyfrig Jones*, W. Calvert†, D. A. Gurnett† & R. L. Huff†

* Space Plasma Physics Group, British Antarctic Survey, Natural Environment Research Council, Madingley Road, Cambridge CB3 0ET, UK
† Department of Physics and Astronomy, The University of Iowa, Iowa City, Iowa 52242, USA

Observations by the Dynamics Explorer 1 satellite provide validation of the theory that terrestrial myriametric radiation is produced by the linear conversion of electrostatic upper hybrid waves to electromagnetic radiation via a radio window. This theory predicts that the myriametric radiation is beamed relative to the magnetic field lines.

TERRESTRIAL myriametric radiation[1] (TMR), also previously referred to as escaping continuum radiation[2], consists of radio waves of wavelength approximately 10^4 m generated predominantly at the plasmapause[3] and magnetopause[4]. At frequencies greater than the magnetosheath plasma frequency (>30 kHz) TMR propagates away into the interplanetary medium, but at lower frequencies it is trapped in the low density region between the plasmasphere and magnetosheath[5] where, after many reflections, it forms a continuum within the magnetospheric cavity. There is strong evidence that the source of TMR lies in electrostatic upper hybrid waves[1-3,6], and numerous theories, both linear[1,7] and nonlinear[8-11], have been proposed for the conversion from electrostatic to electromagnetic waves. One linear theory suggests that the conversion depends on the propagation of upper hybrid waves in density gradients at the plasmapause and magnetopause[1]. If the density gradient is normal to the magnetic field direction, upper hybrid waves can be transformed into electromagnetic Z-mode radiation[12] which is linearly converted to ordinary (O) mode radiation through a radio window[13]. A consequence of this conversion is that the O mode TMR propagates away from the source in two beams at angles with respect to the source magnetic field direction that are dependent on the ratio of electron cyclotron frequency to electron plasma frequency at the window location[1]. Results are presented here of TMR observed with the Dynamics Explorer 1 satellite (DE-1) that for the first time clearly show these two beams. These results demonstrate that the linear Z-mode to O-mode conversion mechanism is operating. A remote sensing technique[14] based on the theory is used to investigate the location and characteristics of the source region. Finally, the location of the TMR source region is demonstrated by direct measurement.

Figure 1 is a frequency-time spectrogram which shows electric field intensities from the plasma wave instrument (PWI) on DE-1. During this interval, the PWI was connected to a 200-m electric dipole antenna located in the spin plane of the spacecraft[15]. The ordinate shows the frequency scale (logarithmic) and the abscissa shows the Universal Time (UT), the magnetic latitude λ, the radial distance (R_E), and the L-value of DE-1. The local electron cyclotron frequency (f_{ce}) is plotted directly on the spectrogram. At frequencies above f_{ce}, and in a very limited latitude range near the magnetic equatorial plane, emissions are seen between the lower harmonics of f_{ce}. These are identified as $(n+1/2)f_{ce}$ electrostatic electron-cyclotron harmonic emissions[16]. The most intense member of this family lies at a higher frequency, $f \approx 62.5$ kHz, which is believed to be the upper hybrid resonance frequency $f_{UHR} = (f_{ce}^2 + f_{pe}^2)^{1/2}$, where $f_{pe} = 9N_e^{1/2}$ Hz is the electron plasma frequency and N_e is the electron concentration in m^{-3}. When DE-1 crossed the equatorial plane, f_{ce} was 7.6 kHz which is much less than f_{UHR}; thus, $f_{UHR} \approx f_p$. This condition would appear to be true for most of the orbit shown. Hence the relatively weak band of noise seen in Fig. 1 in the range 60-100 kHz after 10:30 UT is identified as nonthermal continuum radiation whose lower frequency limit lies near to the value of f_{pe} along the satellite trajectory[5]. After ~11:45 UT, terrestrial kilometric radiation[17] (TKR) can be seen at frequencies above 100 kHz which has propagated to low latitudes from the auroral zones. This radiation tends to be more sporadic and intense than the TMR.

The radiation of interest is seen as two distinct 'blocks' near 100 kHz embedded in the nonthermal continuum on either side of the intense upper hybrid emission recorded at the equatorial crossing, and at a slightly higher frequency. They are seen to be nearly identical and separated by a zone of virtually no emission (except continuum) near the equatorial plane. They are symmetric, but not mirror images, about the equatorial plane and as will be shown shortly are propagating in the directions predicted by the linear Z-mode to O-mode conversion theory[1]. It should also be noted that there is a single block of emission straddling the upper hybrid event right at the magnetic equator which may also be TMR, the satellite in this case possibly being so close to the source that the two beams overlap. This emission is considered in more detail below.

Theory

The linear window conversion theory has been dealt with elsewhere[1,4,13,14,18,19]. It requires that the plasma density gradient ∇N_e in the source region be nearly perpendicular to the magnetic field vector $\mathbf{B}_O$. A result of the conversion is that the O mode electromagnetic radiation is beamed into the low density region in a plane containing ∇N_e and $\mathbf{B}_O$ at two angles, $\beta = \pm\arctan(f_{pe}/f_{ce})^{1/2}$, measured with respect to $\mathbf{B}_O$. If the intense upper hybrid waves are confined to the Magnetic Equator, as they seem to be in this case, the TMR would be beamed with respect to the magnetic equatorial plane at angles of $\alpha = \pm\arctan(f_{ce}/f_{pe})^{1/2}$, one beam to the north and the other to the south.

Thus, if conversion were to occur, the two TMR beams from the intense upper hybrid emission at 62.5 kHz near $\lambda \approx 0°$ in Fig. 1 should make angles of $\pm\arctan(7.6/62.5)^{1/2} = \pm 19°$ with respect to the equatorial plane. Since DE-1 actually passed through the source region for this frequency it was not in a position to observe those particular beams. Their observation would require another satellite in the magnetospheric cavity beyond DE-1 (see Fig. 2).

The two beams of TMR at frequencies above f_{UHR} in Fig. 1 presumably have their sources deeper in the plasmasphere, where the plasma density and hence the corresponding f_{pe} and f_{UHR}, are larger than 62.5 kHz. The decrease of plasma density as DE-1 moved along its trajectory is indicated by the drop in the lower frequency cutoff of the continuum radiation just after 10:30 UT.

Figure 2 shows the magnetic meridian plane trajectory of DE-1 for the period of time represented in Fig. 1. Marked on the trajectory is the point where the intense upper hybrid emission at 62.5 kHz was observed, and the two beams of 62.5 kHz TMR, assuming linear conversion, are shown emanating

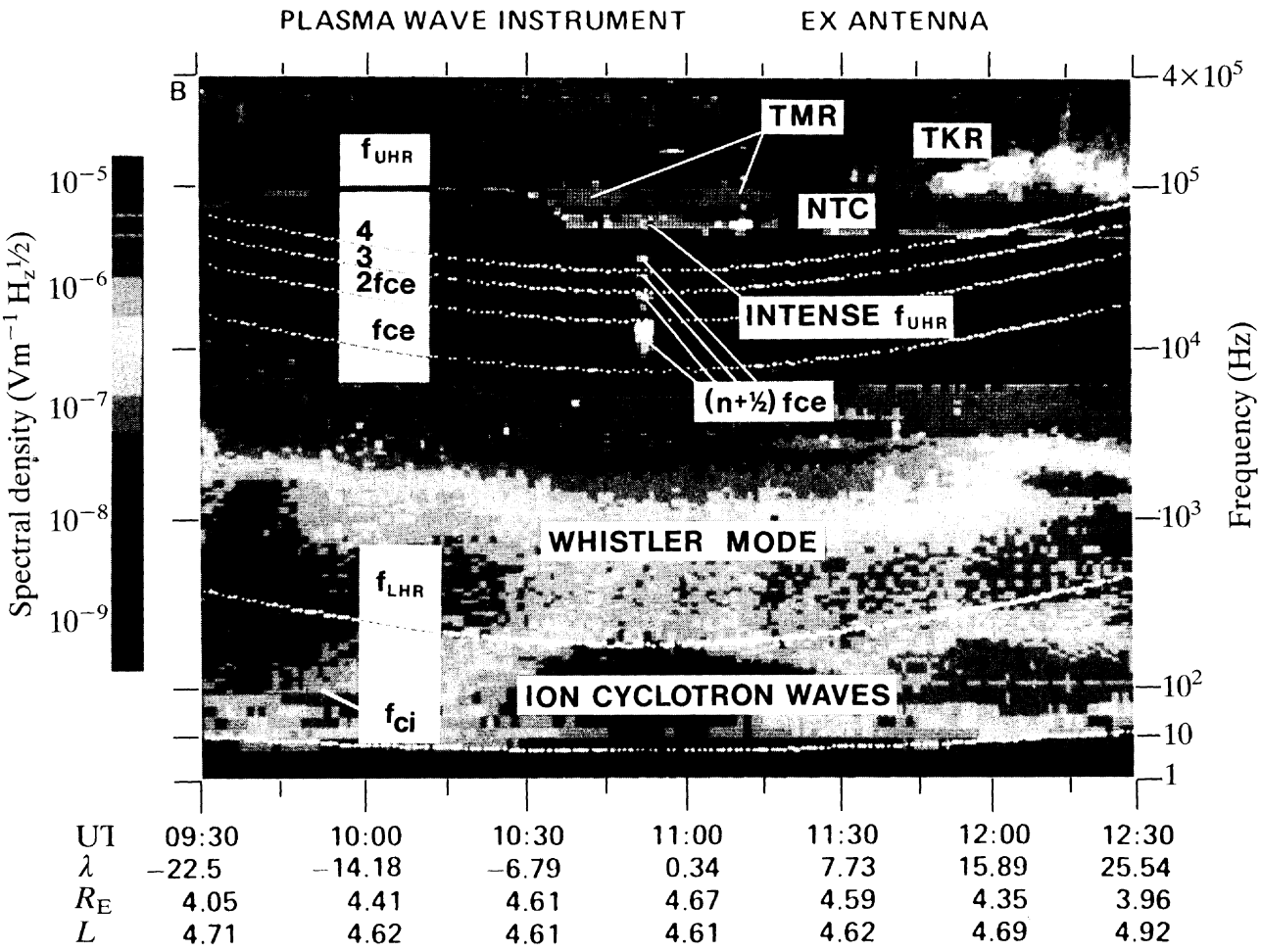

Fig. 1 A spectrogram obtained from the plasma wave instrument on the Dynamics Explorer 1 spacecraft during a south to north pass through the Magnetic Equator.

from it. The location of the source of the upper hybrid emission is slightly south of the Magnetic Equator obtained from the DE-1 magnetic field model. On the basis of this and other evidence[20], we believe that the upper hybrid emission marks the correct location of the actual magnetic equator. Such discrepancies are easily within the range of uncertainty of existing magnetic field models at this radial distance. The magnetic field line labelled $L = 4.665$ shows the field line that would occur if the magnetic equator is adjusted to coincide with location of the upper hybrid emission. As can be seen the satellite trajectory lies virtually along this magnetic field line, especially between 09:30 and 11:30 UT. Thus one would expect this part of the trajectory to be an equipotential and, since it is so close to the Magnetic Equator, to exhibit little variation of the plasma density. However, from the cut-off frequency of the continuum there is clearly a precipitous drop in plasma frequency from 94 kHz ($N_e \approx 1.1 \times 10^8\ m^{-3}$) at 10:27 UT to 58 kHz ($N_e \approx 4.2 \times 10^7\ m^{-3}$) at 10:37 UT. Although the satellite is also moving gradually in longitude, there is unquestionably a very steep density gradient at this time and location. The gradient is not detected north of the equatorial plane presumably because the satellite trajectory remained outside the plasmapause. This is probably one reason why the distribution of continuum and TKR in Fig. 1 is also not symmetrical about the Equator.

Remote sensing

The relationship $\beta = \pm\arctan\,(f_{pe}/f_{ce})^{1/2}$ allows one to demonstrate that the two beams of TMR in Fig. 1 were most probably produced by the linear Z-mode to O-mode conversion mechanism. A form of remote sensing can be used to determine the

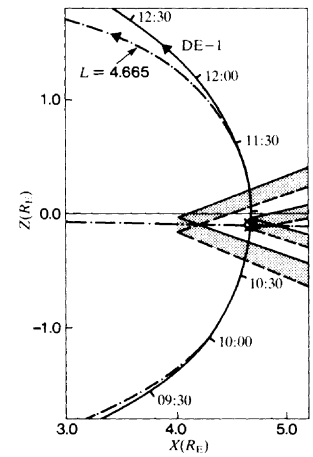

Fig. 2 The trajectory of DE-1 (curved full line) during the time when the data in the spectrogram in Fig. 1 were recorded. The model and corrected magnetic equators (full and chained lines respectively) are shown. The chained line labelled $L = 4.665$ represents a magnetic field model that has been adjusted such that the field line passes through the UHR emission at the Magnetic Equator. Hypothetical sources and beams of TMR are shown. The outer beam pair is presumed to emanate from the 62.5 kHz UHR emission at $4.665 R_E$. Observation of these beams would require another satellite outside the trajectory of DE-1. The inner beam pair is assumed to be at a frequency of 100 kHz and to have its source at $4 R_E$. In both cases the sources have a small latitudinal extent about the Magnetic Equator.

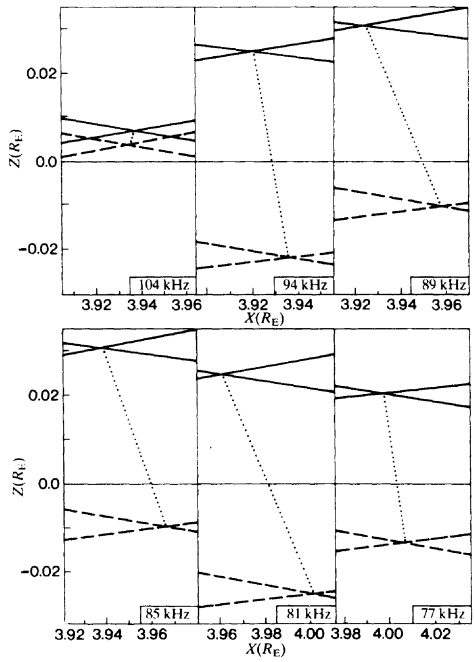

Fig. 3 Source location (dotted lines) of the TMR at 77 kHz to 104 kHz obtained by remote sensing. Negative sloping broken and full lines are possible source positions of the southern beam, whereas the positive sloping broken and full lines are corresponding source locations for the northern beam.

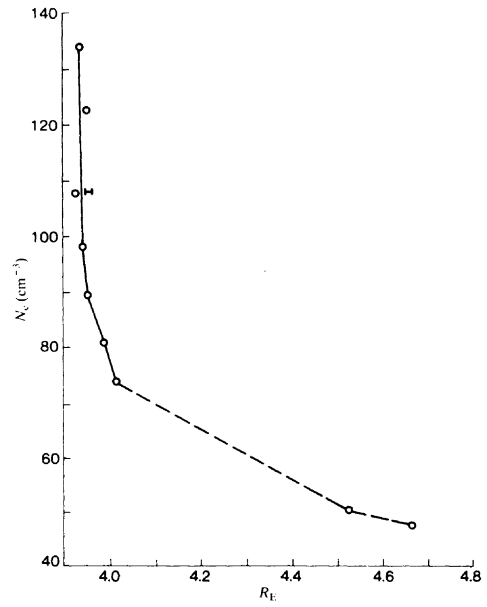

Fig. 4 An approximate plasma density profile (full line) deduced from Fig. 3. The dashed line connects the profile to the points obtained from the TMR identified at 64 kHz (see Fig. 5) and the UHR emissions observed at $4.665R_E$. The bar at $N_e = 109\ \text{cm}^{-3}$ shows the magnitude of the error in the source position as estimated from Fig. 3.

position of the TMR sources at the different frequencies. This technique has been described in detail elsewhere[14] and only a brief outline will be given here.

Given that TMR of frequency f is emitted where $f = f_{pe}$ and that it is beamed with respect to the source magnetic field at an angle which depends on f_{pe} and f_{ce}, one may determine, for a given magnetic field model, where an observer has to be located in order to receive the radiation. Conversely, knowing the magnetic coordinates of the observer one can determine the possible positions of the sources in a magnetic field model. For the Earth, it may be assumed that the magnetic field is dipolar within about $4R_E$. If one concentrates on possible sources in the vicinity of the equatorial plane, the location and dimension of the TMR source in Fig. 1 can be determined. It is assumed here that propagation is in the magnetic meridian plane. Consider, for example in Fig. 2, a source of 100 kHz having a magnetic field-aligned latitudinal extent of 2° centred on the equatorial plane and located at $4R_E$. The cyclotron frequency is assumed to be 12 kHz. Thus $\beta \approx 70°$ and the two beams should appear as shown in the figure. As DE-1 moves northwards towards the equator it observes the southern beam, first encountering the radiation from the southern edge of the source and then encountering the radiation from the northern edge of the source. As the satellite continues northwards past the Equator and into the Northern Hemisphere, it observes the northern beam, again receiving first the radiation from the southern edge of the source and then the radiation from the northern edge. If the source is not exactly uniform with latitude it is clear that the satellite would observe, not a mirror image about the equatorial plane, but a sequential repetition of the non-uniformities as it progresses northwards through the two beams. This repetition is clearly visible for the two blocks of TMR appearing in Fig. 1.

The remote sensing technique was applied to the beam edges at different frequencies in Fig. 1 to investigate the source positions and dimensions, and the results are presented in Fig. 3 which shows the source locations of TMR for six frequencies ranging from 77 kHz to 104 kHz. The abscissae X represent the radial distance in the equatorial plane and the ordinates Z the distance normal to that plane. Each panel has a pair of dashed lines and a pair of full lines. The lower, negatively-sloping dashed lines represents possible source locations for the lower edge of the southern beam, whereas the upper positively-sloping dashed lines give the possible source positions for the lower edge of the northern beam. As was stated earlier, these beam edges should have originated from the same part of the source, namely its southern edge. Therefore where the two dashed lines intersect should yield the position of the southern edge of the source, whereas where the two similarly-deduced full lines intersect should give the location of the northern edge of the source. Thus the apparent sources determined by this remote sensing technique for the different frequencies are represented by the dotted lines connecting these two intersections. Clearly there is a considerable variation in their dimensions extending from only $\sim 0.0025R_E$ (16 km) at 104 kHz to $\sim 0.05R_E$ (320 km) at 81 kHz. The sources are not magnetic field-aligned normal to the equatorial plane, and this is most probably due to inaccuracies in determining precisely the Magnetic Equator or the beam edges, or to temporal and spatial variations of the plasmapause during the 15-min interval between the measurements. It may also be that the density gradient is not exactly radial during the time period involved, so that the beams are not emitted strictly in the magnetic meridian.

For each of the frequencies in Fig. 3 the mean source location can be used to obtain an approximate plasma density profile of the plasmapause, since the theory states that $f = f_p = 9(N_e)^{1/2}$. The result is shown in Fig. 4 which clearly implies a very steep density gradient between $3.93R_E$ and $4R_E$ which would be conducive to mode conversion according to the linear theory. Although this density gradient cannot be associated directly with that suggested from the sharp decrease in f_{pe} at 10:27 UT and $L \approx 4.665$, it is compatible with the existence further in of a very steep plasmapause at this time.

Attention was drawn earlier to the emission, tentatively identified as TMR, near to and straddling the upper hybrid waves at the magnetic equator. The result of remote-sensing using the two edges of this emission at $f = 64$ kHz is shown in Fig. 5. The

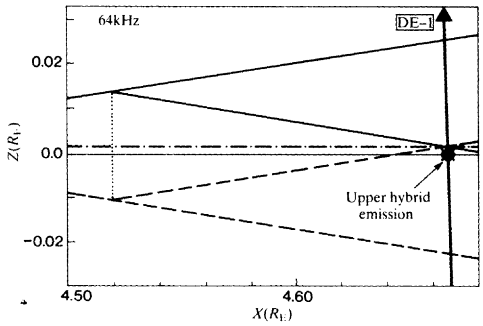

Fig. 5 Remote sensing of the edges of the continuous 'block' of TMR at 64 kHz. The dashed lines represent the beams from the southern source edge and the full lines the beams from the northern edge. A source at radial distance less than $4.52R_E$ would have resulted on the observation of two distinct beams.

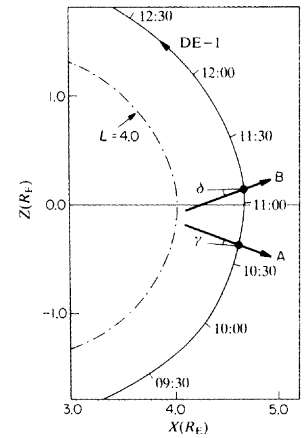

Fig. 7 The wave directions deduced from Fig. 6, along with the DE-1 orbit and the $L=4$ L-shell from which the emissions seem to have originated.

trajectory of DE-1 and the position of the 62.5 kHz upper hybrid emission (at the corrected Magnetic Equator) are illustrated. The possible source positions of the 64 kHz TMR lie on the negatively-sloping dashed line (southern edge of possible source) and positively-sloping full line (northern edge of possible source). If it is assumed that the source is normal to the Magnetic Equator, then the minimum radial distance of the source would be $4.52R_E$. Source locations at a smaller radial distance would result in DE-1 observing two separate beams with a zone of no emission in between. This source location and corresponding plasma density were included in Fig. 4, along with the density determined from the upper hybrid emission at $4.665R_E$. They are joined to the other points by dashed lines to emphasize that the $4.52R_E$ source at 64 kHz is only an inner limit, assuming that the emission was actually TMR. A possible reason for the absence of TMR at frequencies between 64 kHz and 77 kHz may be that the density gradient is not sufficiently large for the conversion mechanism to operate efficiently.

Measured wave directions

The intensity of the TMR in Fig. 1 is, before smoothing, found to be strongly modulated by the rotation of DE-1's electric dipole antenna. For compact sources near the spin plane of the antenna, the modulation pattern, as a function of the antenna rotation angle, should be characterized by distinct nulls from which the wave direction can be determined[21]. The DE-1 spacecraft spins in a 'reverse-cartwheel' mode, with its spin axis oriented perpendicular to the orbit plane. Because of this orientation, and also because the satellite's orbit plane lies nearly in the magnetic meridian, the geometry is ideal for spin-null direction-finding measurements, thereby providing us with an opportunity to test the linear conversion model by making direct measurements.

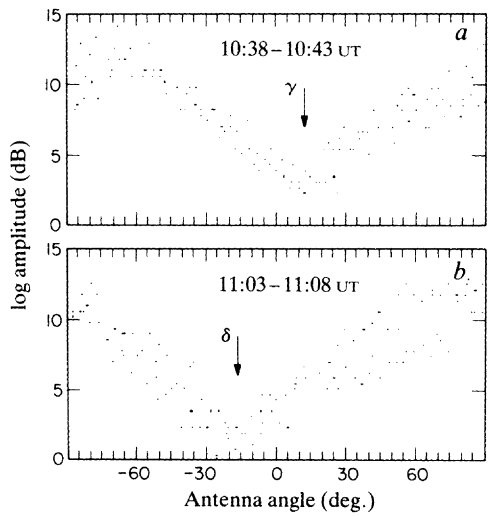

Fig. 6 Amplitudes of the TMR signals in Fig. 1 as a function of the DE-1 antenna angle, measured with respect to nadir at the times and frequencies indicated. The relatively deep nulls at angles γ and δ give the wave ray directions shown plotted in Fig. 7.

Figure 6 shows the measured electric field intensities as a function of the antenna angle with respect to the spacecraft-Earth line (nadir direction) projected into the spin plane, with panels *a* and *b* pertaining to the two blocks of TMR discussed above. In both cases pronounced spin nulls were clearly evident. The angles γ and δ presumably correspond to antenna alignment with the propagation direction, since the wave electric field in this case should be almost perpendicular to the wave direction. The two angles γ and δ, on opposite sides of the spacecraft nadir before and after the apparent equatorial crossing, thus measure directly the wave directions for the two components of TMR.

Figure 7, in the same format as Fig. 2, shows these wave directions at the locations where they were observed. As predicted, the two directions were approximately symmetric on opposite sides of the emission axis and in excellent agreement with those deduced from the linear conversion model. Moreover, the apparent source location, near $L=4$ and 85 kHz, is also consistent with the plasmapause position deduced from the remote sensing technique described in the previous section. The theoretical model, therefore, is not only internally consistent with the detection of TMR beams where they were observed, but also directly confirmed by the spin-null direction-finding measurements.

Conclusions

The observations presented here strongly support the picture of TMR beaming which is predicted by the linear Z-mode to O-mode conversion theory. Taken with the evidence that the conversion mechanism also seems to be operative in the magnetospheres of Jupiter[22] and Saturn[23], it would appear that the process may also be of importance in a wider, astrophysical context.

Investigation of this and other similar events is continuing. In particular, the possibility that the emissions derive from a non-radial density gradient is under study. Also the theory predicts that the southern TMR beam should be right-hand

polarized, whereas the polarisation of the northern beam should be left-handed. Although the PWI can sometimes measure wave polarization directly, the TMR emissions in this case were too weak for a reliable polarization analysis. We are currently searching for more intense TMR events, for which a polarization analysis is possible, and the results of such polarization measurements and other studies will be reported separately.

We thank R. C. Olsen for bringing this event to our attention and for supplying the original (colour) version of the spectrogram in Fig. 1 (see ref. 24). The research at the University of Iowa was supported by NASA and by the Office of Naval Research.

Received 30 March; accepted 8 June 1987.

1. Jones, D. *Nature* **288**, 225-229 (1980).
2. Gurnett, D. A. *J. geophys. Res.* **80**, 2757-2763 (1975).
3. Gurnett, D. A. *J. geophys. Res.* **81**, 3875-3885 (1976).
4. Jones, D. *Planetary Radio Emissions* (eds Rucker, H. O. & Bauer, S. J.) 11-57 (Osterreichische Akademie der Wissenschaften, Vienna, 1985).
5. Shaw, R. R. & Gurnett, D. A. *J. geophys. Res.* **78**, 8136-8149 (1973).
6. Kurth, W. S. *Geophys. Res. Lett.* **9**, 1341-1344 (1982).
7. Ashour-Abdalla, M. & Okuda, H. *J. geophys. Res.* **89**, 9125-9131 (1984).
8. Melrose, D. B. *J. geophys. Res.* **86**, 30-36 (1981).
9. Ronnmark, K. *Ann. Geophys.* **1**, 187-192 (1983).
10. Christiansen, P. J. *et al. Geophys. Res. Lett.* **11**, 139-142 (1984).
11. Ronnmark, K. *Geophys. Res. Lett.* **12**, 639-642 (1985).
12. Oya, H. *Planet. Space Sci.* **22**, 687-708 (1974).
13. Jones, D. *Nature* **260**, 686-689 (1976).
14. Jones, D. *J. Geophys.* **52**, 158-166 (1983).
15. Shawhan, S. D. *et al. Space Sci. Instr.* **5**, 535-550 (1981).
16. Kennel, C. F. *et al. J. geophys. Res.* **75**, 6136-6152 (1970).
17. Gurnett, D. A. *J. geophys. Res.* **79**, 4227-4238 (1974).
18. Budden, K. G. & Jones, D. *Ann. Geophys.* **5A**, 21-28 (1987).
19. Jones, D. *Physica scripta* **35**, 887-894 (1987).
20. Gough, M. P. *et al. Nature* **279**, 515-517 (1979).
21. Kurth, W. S. *et al. J. geophys. Res.* **80**, 2764-2770 (1975).
22. Jones, D. *Nature* **324**, 40-42 (1986).
23. Jones D. *Nature* **306**, 453-456 (1983).
24. Olsen, R. C. *et al. J. geophys. Res.* **92**, 2385-2407 (1987).